Spatiotemporal Distance Class Analysis of Plant Disease Epidemics

Scot C. Nelson

Assistant professor, University of Hawaii at Manoa, Department of Plant Pathology, Honolulu 96822.
This work was supported by the University of Hawaii Office of Research Administration.
University of Hawaii College of Tropical Agriculture and Human Resources Journal Series 3931.
I thank S. A. Ferreira and K. Y. Pitz, University of Hawaii, Department of Plant Pathology, for assistance with papaya ringspot data collection and analysis and R. D. Berger, University of Florida, Department of Plant Pathology, for data provided from an epidemic of citrus variegated chlorosis in Brazil.
Accepted for publication 21 September 1994.

ABSTRACT

Nelson, S. C. 1995. Spatiotemporal distance class analysis of plant disease epidemics. Phytopathology 85:37-43.

Spatiotemporal distance class analysis is proposed as a new form of spatiotemporal analysis of intensively mapped, binary data. The method detects and quantifies attributes of nonrandom patterns of disease increase in regularly spaced plant populations. The method tests the hypothesis that healthy plants in a population have an equal (random) chance of becoming diseased in the period between two disease assessment dates. Mapped disease incidence evaluations from two assessment dates are needed for the analysis. Expected spatial patterns of diseased plants for the second assessment date are generated by assigning the number of newly diseased plants to random spatial positions among the healthy plant population observed on the first assessment date. Distance class analysis techniques are used to compare these expected patterns with the actual spatial pattern observed on the second assessment date. The number, location, and configuration of significant distance classes are used to evaluate the randomness of the observed spatial distribution. Hypothetical examples and data from an epidemic of citrus variegated chlorosis in Brazil and an epidemic of papaya ringspot in Hawaii are presented to illustrate the procedure.

Two-dimensional distance class analysis was developed originally by Gray et al (6) to quantify spatial aspects of plant virus epidemics in regular lattices of host plants. Guidelines for its use and interpretation were improved and evaluated (11,12). Applications of two-dimensional distance class analysis have proved useful in the analysis of binomial spatial data from a number of bacterial, fungal, and viral pathosystems (3,4,7, 9–11,15).

A significant limitation of the two-dimensional distance class method is that analysis of pattern is restricted to single dates of observation. Therefore, hypotheses concerning attributes of disease increase cannot be tested directly. These spatial and temporal attributes can be only inferred or recognized indirectly from sequentially performed analyses.

Methodology based upon autocorrelation and time-series analyses has been applied successfully to spatiotemporal disease incidence data (13,14). These studies, however, required disease assessments be made for subpopulations of plants located within quadrats. Few distance-based procedures have been available for analysis of spatiotemporal increase of disease incidence in a population of individual plants. A more complete understanding of epidemics may be dependent upon the ability of investigators to test specific hypotheses about plant-to-plant patterns of disease increase. Therefore, a method for directly assessing spatiotemporal changes in patterns of disease presence or absence among individuals in a population could be a valuable tool for augmenting our knowledge of pathosystems. The purpose of this paper is to introduce spatiotemporal distance class analysis, a method for evaluating and quantifying the randomness of the increase in newly diseased plants from one assessment date to the next.

MATERIALS AND METHODS

Model assumptions and hypothesis. The spatiotemporal distance class model assumes that disease incidence data (presence or absence) are collected from a regular lattice or matrix of sampling units (rows and columns) and that diseased units (e.g., plants and quadrats) remain diseased between two disease assessments. Spatial locations of diseased units within the lattice are defined by their X (row) and Y (column) coordinates with a total of m diseased units observed on the first assessment date and a total of n diseased units that become diseased between the first and second assessment dates. Spatiotemporal distance class analysis tests the hypothesis that the n diseased units are distributed randomly within the lattice. If this hypothesis is rejected, then attributes of the nonrandom patterns can be described (e.g., average $[X, Y]$ distance of newly diseased units from previously diseased units, directional increase of disease, and establishment of secondary foci).

The basis for hypothesis testing in spatiotemporal distance class analysis is the statistical comparison of an observed lattice with computer-generated "expected patterns" of disease increase. Within a lattice of the same dimensions as the observed data, expected patterns are generated that have m diseased units in the same $[X, Y]$ coordinates as in the observed lattice but have n newly diseased units that are randomly assigned with a pseudo-random number generator (12) to previously nondiseased coordinates. Four hundred expected maps are generated for each observed data set.

Standardized count frequencies. Significance testing in spatiotemporal distance class analysis is based on the comparison of a standardized count frequency (SCF) calculated for each observed $[X, Y]$ distance class with similar SCFs computed from the expected patterns. An SCF is based on a tabulation of the number of times that diseased units are separated by a given $[X, Y]$ distance. The total number of $[X, Y]$ distance classes equals the (row $\times$ column) dimensions of the observed lattice.

Calculation of SCF values begins at one corner of the observed lattice with a systematic search for the first diseased unit, termed "reference unit 1." Once located, it is assigned an $[X, Y]$ coordinate. Each of the remaining $(m + n) - 1$ diseased units within the lattice is also mapped to an $[X, Y]$ coordinate. The $[X, Y]$ distance separations (i.e., distance classes) between each of the $(m+n) - 1$ diseased units and reference unit 1 are calculated

by the absolute differences in their X and Y coordinate values: $[|X_1 - X_i|, |Y_1 - Y_i|]$, where X_1 and Y_1 represent the X and Y coordinate values, respectively, for reference unit 1, and X_i and Y_i ($i = 2, 3, \ldots, [m + n]$) are the X and Y coordinates in the lattice for the remaining $(m + n) - 1$ diseased units in the lattice, respectively. The process of locating each $(m + n) - 1$ diseased unit, assigning it an $[X, Y]$ coordinate, calculating the $[X, Y]$ distance class between it and reference unit 1, and incrementing the "count frequency" (i.e., the number of times that two diseased units are separated by a given distance class) is repeated until all $(m + n) - 1$ diseased units are identified and compared with reference unit 1. This procedure is then repeated until each of the $(m + n)$ diseased units is used as a reference unit. Subsequently, the observed count frequency for each distance class is standardized by dividing by the total number of possible unit pairs in each respective distance class. SCF values for distance classes from each of the 400 expected patterns are calculated similarly.

Significance of the observed SCF for each $[X, Y]$ distance class is determined by calculating the percentage of times it exceeds or is exceeded by the 400 expected pattern SCFs tabulated for the same distance class. If the value of the observed SCF exceeds the expected SCF values >95% of the time, the SCF is deemed significantly greater than expected ($P \leq 0.05$). Thus, more diseased unit pairs are separated by that $[X, Y]$ distance than would be expected with a random occurrence of newly diseased units. Similarly, when the value of the observed SCF exceeds the expected pattern values <5% of the time, the SCF is deemed significantly less than expected ($P \geq 0.95$).

The distance class matrix. The significance of SCF values is summarized in a "distance class matrix." The proportion of significant SCF values relative to matrix size is an indication of the degree of nonrandomness in the observed data. The relative size, shape, and position of contiguous groups of significant SCF values within the distance class matrix are used to describe and quantify attributes of pattern. Of particular interest are characteristics of the "core cluster" and "reflected clusters" within the distance class matrix.

Core clusters represent the average or typical organization of newly diseased units in relation to previously diseased units. The core cluster is defined as the group of contiguous, significant ($P \leq 0.05$) SCF values for distance classes adjacent to the $[X, Y]$ region [0,0] of the distance class matrix. For patterns of disease increase in units closely associated to previously diseased units, the core cluster is expected to be relatively large and discrete.

To summarize the intensity of aggregation of newly diseased units, a "proximity index" was defined as the ratio of the number of significant SCF values ($P \leq 0.05$) in a core cluster to the $[X, Y]$ dimensions of the core cluster. For the denominator, the $[X, Y]$ dimensions of the core cluster are determined by locating the maximum distance from the [0,0] distance class to which contiguous, significant ($P \leq 0.05$) SCF values extend in both the X and Y directions. Thus, the proximity index is a measure of the relative density of significant SCF values within the core cluster.

Values for the proximity index range from a minimum value near zero to a maximum value of 1.0 for rectangular core clusters (i.e., when the number of significant SCF values in the cluster equals its $[X, Y]$ dimensions) (Fig. 1). When nonrandom disease increase occurs to adjacent units, the value for the proximity index is expected to approach 1. The value of the index is expected to approach a minimum value for nonrandom disease increase. The minimum values of the index are found for core clusters of diagonal shape, e.g., extending from the $[X, Y]$ distance class [0,0] to [1,1], [2,2], [3,3] . . . $[X_i, Y_i]$, where $[X_i, Y_i]$ represent the X and Y dimensions of the core cluster, respectively. Statistical significance levels are not assigned to values of the proximity index, but replicate values could be submitted to analysis of variance. Hypothetical examples of core clusters with identical $X \times Y$ dimensions but with different values for the proximity index are provided (Fig. 1).

Contiguous groups of significant ($P \leq 0.05$) SCF values elsewhere in the distance class matrix are known as reflected clusters, which may indicate disease increase in secondary foci.

Analytical guidelines. Guidelines and criteria similar to those recommended for two-dimensional distance class analysis were adopted for spatiotemporal distance class analysis (6,11,12). Disease incidence on the first assessment date must be ≥1%. The percentage of newly diseased units observed on the second assessment date must be 10–90% of the remaining nondiseased population. The maximum missing values for an observed data set is 20%. A minimum of 400 expected data sets is compared with each observed data set. Slight variability in significance of SCF values is expected to occur when the same data are analyzed repeatedly because of differing randomizations in the expected patterns. Diseased units must remain diseased throughout the entire epidemic or, if rogued or absent, are rated as missing.

Relatively conservative guidelines were developed for interpretation of the distance class matrix. The minimum total significant SCFs (i.e., the total of those at $P \leq 0.05$ and those at $P \geq 0.95$) required to indicate a nonrandom pattern of disease increase is 5% of the total number of distance classes. Data sets with >8% significant SCF values are interpreted to be strongly nonrandom. Edge effects are significant if ≥12.5% of the SCF values at the right hand (X_{max}) and bottom (Y_{max}) edges of the distance class matrix are significantly greater than expected ($P \leq 0.05$).

Hypothetical example. A hypothetical example consisting of two sets of arbitrarily fabricated data was created to introduce the analysis and to demonstrate interpretation of nonrandom and "nearly random" patterns of disease increase in 10 × 10 plant lattices (Fig. 2). On the first assessment date, the data sets had identical disease foci, each consisting of a single, rectangular cluster of 24 diseased plants in a corner of the lattice (Fig. 2A

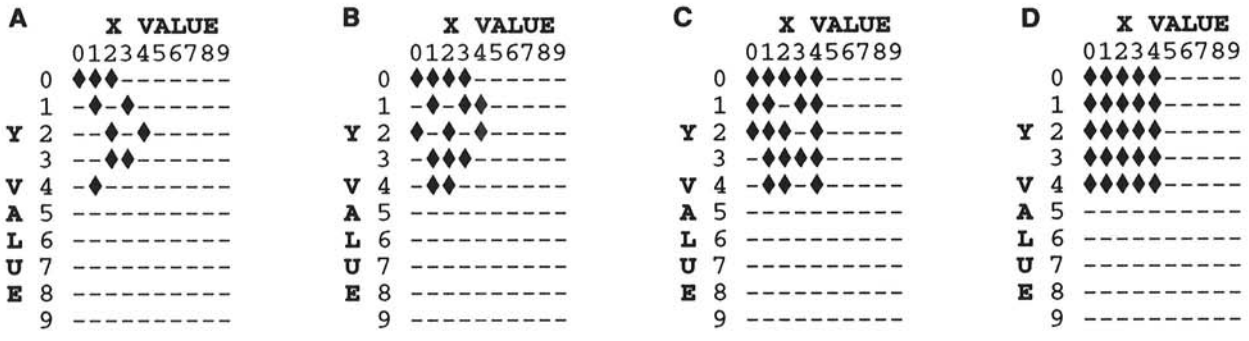

Fig. 1. Hypothetical distance class matrices from analysis of spatiotemporal patterns in 10-row × 10-column plant lattices. The four distance class matrices (**A, B, C, and D**) have core clusters of different sizes: 10, 15, 20, and 25 significant standardized count frequencies (SCF), respectively ($P \leq 0.05$) within identical $X \times Y$ core cluster dimensions (i.e., 5 × 5). Values for the proximity index for **A–D** are 0.4, 0.6, 0.8, and 1.0, respectively. ◆ = $[X, Y]$ distance class with SCF significantly greater than expected ($P \leq 0.05$), and − = $[X, Y]$ distance class with nonsignificant SCF value.

and C), but they differed in the $[X, Y]$ locations of 14 newly diseased plants on the second disease assessment date. For the nonrandom pattern of disease increase, newly diseased plants were placed in close proximity and/or adjacent to previously diseased plants. For the nearly random pattern of disease increase, newly diseased plants were located distal to previously diseased plants and showed no marked or consistent spatial relationship with them or with each other (Fig. 2C).

Analysis of actual epidemics. Spatiotemporal data from two epidemics were obtained: 1) citrus variegated chlorosis on citrus, observed during 1989–1992 in Brazil and 2) papaya ringspot on papaya (*Carica papaya*), observed during 1992–1993 on the island of Oahu, Hawaii. The examples were chosen to demonstrate a direct and an indirect approach for analysis of disease increase attributes in actual epidemics.

Citrus variegated chlorosis. Since 1987, citrus variegated chlorosis, a new sweet orange (*Citrus sinensis*) decline disease, has spread rapidly in some states in Brazil (5,8). A xylem-limited bacterium (*Xylella fastidiosa*) was a reported causal agent (2). The most striking symptoms are the very small, yellow, acid fruit. Foliar and fruit symptoms may be restricted to only one or two branches on a tree; but in severe cases, all branches may be affected.

Data were available from an epidemic of citrus variegated chlorosis in a Brazilian orange grove planted in 1983. Trees were cultivar Natal sweet orange on Cleopatra mandarin (*C. reshni*) rootstocks. In the grove, between-row spacing was 8 m, and within-row spacing of trees was 6 m. From 1989 to 1992, yearly maps of incidence of citrus variegated chlorosis in the grove were produced (Fig. 3A, C, and E). Disease incidence was assessed by observing visually diagnostic symptoms of citrus variegated chlorosis. A subset of the data was selected for analysis (12 rows × 77 plants per row). This subset included the initial disease focus in the grove.

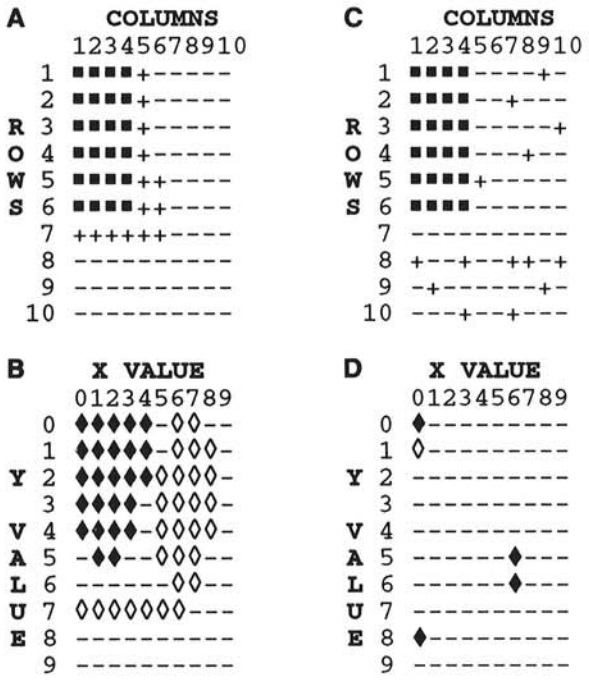

Fig. 2. Maps of two hypothetical data sets and corresponding distance class matrices depicting analysis of nonrandom and nearly random increase of disease between two disease assessment dates. **A and C,** Maps of nonrandom disease increase and nearly random disease increase, respectively. ■ and + = diseased plant on first and second disease assessment dates, respectively; and − = nondiseased plant. **B and D,** Distance class matrices from spatiotemporal distance class analysis of the data in **A** and **C,** respectively. ◆ = $[X, Y]$ distance class with standardized count frequency (SCF) significantly greater than expected ($P \leq 0.05$); ◇ = $[X, Y]$ distance class with SCF significantly less than expected ($P \geq 0.95$); and − = $[X, Y]$ distance class with nonsignificant SCF value.

Papaya ringspot. Incidence of the viral disease papaya ringspot was mapped monthly in two commercial plantings (approximately 6 ha) of papaya at Punaluu, Oahu, for 12 mo beginning in September 1992. The adjacent fields were located in a valley in which there were no other commercial plantings of papaya. The papaya fields were separated by a windbreak of *Adenanthera pavonina* (false wiliwili) trees more than 10 m tall. In one field, plants were arranged in an approximately regular lattice of 24 rows and 32 plants per row. Row spacing was 3.5 m with 2 m between plants. Trees were approximately 12 mo of age when disease assessments began. On each assessment date, each plant was inspected visually for diagnostic symptoms of papaya ringspot (i.e., leaf mosaic, water-soaked streaking of petioles, and ring spots on fruit). Diseased trees were identified, tagged, and rogued by the farm manager.

For the purpose of illustration, a 20-row × 24-column subset of the data is presented (Fig. 4). This was done to reduce the proportion of missing values and to increase values for disease incidence (in accordance with the analytical criteria and guidelines). Similarly, low values for increase in percent disease between consecutive disease assessment dates disallowed a direct analysis of disease increase for those assessment intervals. Alternatively, indirect analyses were conducted that utilized overlapping disease assessment intervals. To illustrate, assume three disease assessment times, t_1, t_2, and t_3. Suppose that the assessment interval of direct interest was from t_2 to t_3 but that a low value for percent disease increase (e.g., 2%) between these dates disallowed direct application of spatiotemporal distance class analysis to this interval. A comparison of distance class matrices from an overlapping analysis of disease increase from t_1 to t_2 and from t_1 to t_3 was expected to provide evidence of spatiotemporal attributes of disease increase between t_2 and t_3. Similarly, an alternative approach was conducted for other assessment intervals whereby the reference date (e.g., t_3) was held constant while previous dates were allowed to vary.

RESULTS

Hypothetical example. The distance class matrices for the hypothetical example revealed distinct differences between nearly random and nonrandom disease increase between t_1 and t_2 (Fig. 2B and C). In the nonrandom example, there were 24 of 99 (24.2%) $[X, Y]$ distance classes (excluding the $[X, Y]$ class [0,0]) with SCF values significantly greater than expected ($P \leq 0.05$). The spatial organization of these significant distance classes revealed the nonrandomness. The presence of a relatively large and discrete core cluster in the approximate $[X, Y]$ region [0–4,0–4] was taken as direct evidence that increase of disease was likely to occur in close proximity to previously diseased plants. Also, there was a contiguous and discrete group of $[X, Y]$ distance classes with SCF values significantly less than expected ([6–7,0], [6–9,1], [5–8,2–4], [5–7,5], [6–7,6], and [0–5,7]) ($P \geq 0.95$) (Fig. 2B). A group of SCFs of this type was interpreted as reflecting potential spatial limits of disease increase or an area or zone within the field in which the occurrence of newly diseased plants was uncommon. When disease increase was nearly random (Fig. 2C), only three SCF values within the distance class analysis matrix were significantly greater than expected (Fig. 2D), and the core cluster size was equal to 1 (the minimum possible size).

Citrus variegated chlorosis. Increase of citrus variegated chlorosis from 1989 to 1990 was strongly nonrandom (Table 1, Fig. 3A and B). The large core cluster indicated that the spatial location of newly diseased plants occurred almost exclusively in close proximity to previously diseased plants. Within-row disease increase and cluster expansion were evident on up to 17 trees within a row and for the entire width of the lattice (12 columns) (i.e., the $X \times Y$ dimensions of the core cluster). Additional evidence for nonuniform increase of disease was indicated by a large group of distance classes with SCFs significantly less than expected ($P \geq 0.95$) within the distance class matrix. The approximate $[X, Y]$ coordinates for this group were [26–49,0–6] (Fig. 3B). The increase of citrus variegated chlorosis between 1990 and 1991 also was

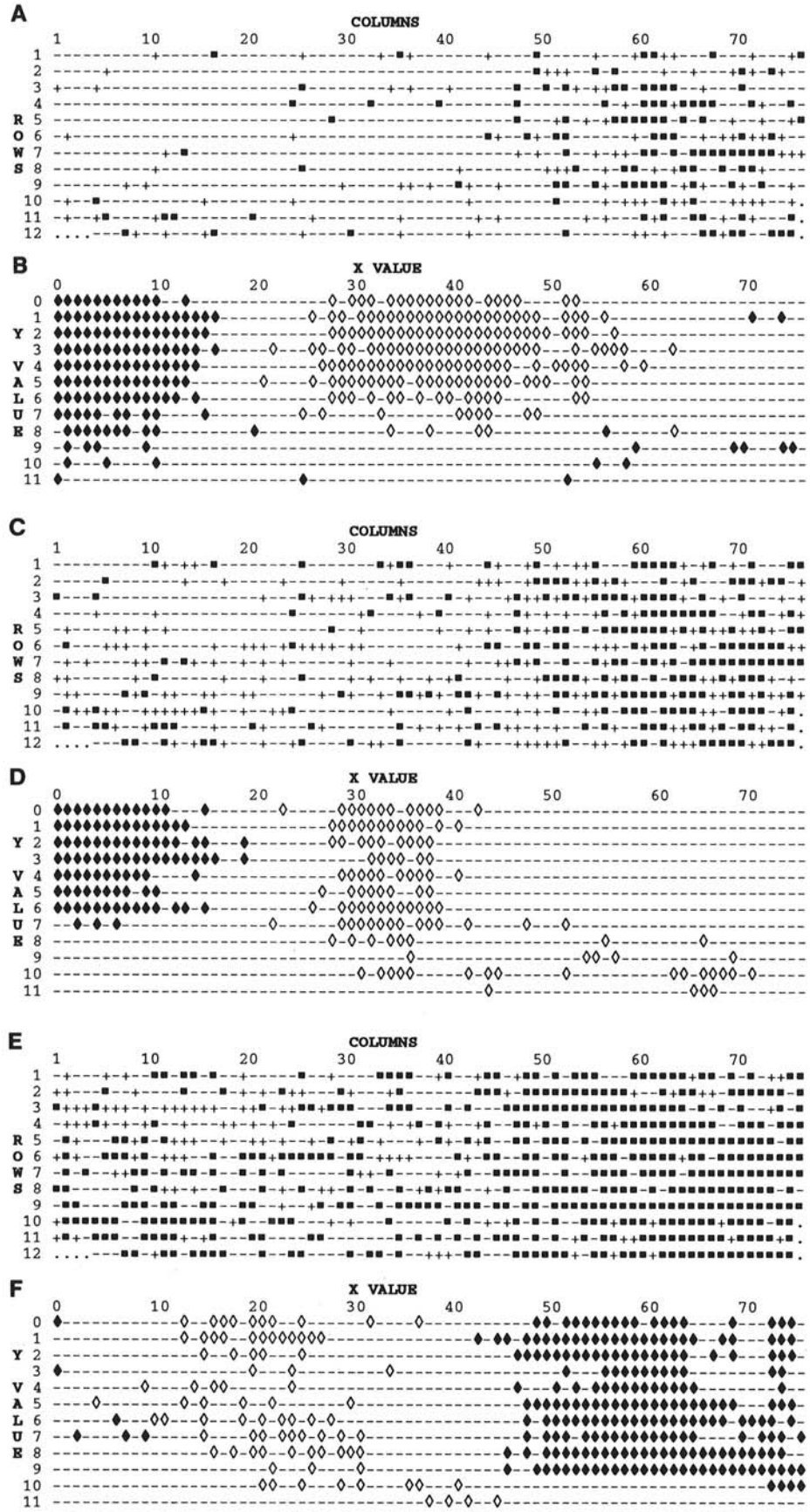

Fig. 3. Spatiotemporal distance class analysis of an epidemic of citrus variegated chlorosis in Brazil during 1989–1990. **A, C, and E,** Maps of disease increase from 1989 to 1990, 1990 to 1991, and 1991 to 1992, respectively. ■ and + = diseased plant on first and second disease assessment dates, respectively, for each assessment interval; and − = nondiseased plant. **B, D, and E,** Distance class matrices from spatiotemporal distance class analysis of data in **A, C, and E,** respectively. ◆ = $[X, Y]$ distance class with standardized count frequency (SCF) significantly greater than expected ($P \leq 0.05$); ◇ = $[X, Y]$ distance class with SCF significantly less than expected ($P \geq 0.95$); and − = $[X, Y]$ distance class with nonsignificant SCF value.

strongly nonrandom (Table 1, Fig. 3C and D). The size of the core cluster was reduced from the previous disease assessment interval (1989–1990), yet the relatively high value for the proximity index still indicated that newly diseased plants occurred in close proximity to previously diseased plants. In the assessment period from 1991 to 1992, direct evidence for increase of disease in close proximity to previously diseased trees was not detected; the core cluster size was 1 (Table 1, Fig. 3E and F). Indirect evidence, however, for continued localized increase of disease and/or continued cluster expansion was the presence of a reflected cluster in the distance class matrix (Fig. 3F). This cluster was defined by the area within the approximate $[X, Y]$ coordinates [46–75, 0–10]. These data were taken as evidence that the increase of disease from 1991 to 1992 occurred primarily near secondary disease foci.

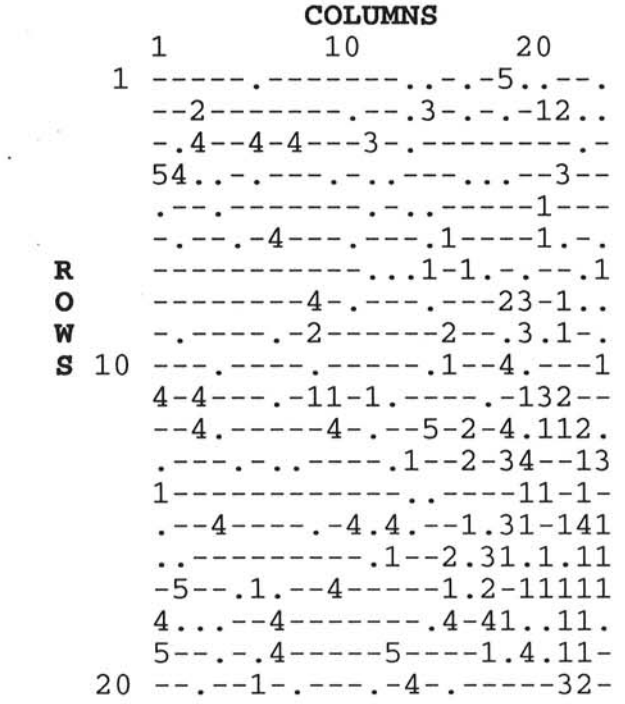

Fig. 4. An epidemic of papaya ringspot in Hawaii. Map of healthy, missing, and diseased plants in a 20-row × 24-column subset of data from a commercial field of papayas at Punaluu, Oahu, during 1992–1993. 1-5 = Plant diseased with papaya ringspot in November 1992, February 1993, March 1993, July 1993, or August 1993, respectively; − = healthy plant; and . = missing value or dead plant.

Papaya ringspot. Increase of papaya ringspot was strongly nonrandom during each of the disease assessment intervals (i.e, significant distance classes exceeded 8%). The size of the core cluster within the distance class matrix and its shape and organization indicated that increases in disease from November to July and from November to August were likely to occur in close proximity to previously diseased plants (i.e., generally within five to six plant rows and nine to 11 plants within rows) (Table 1, Figs. 4 and 5A and B). The presence of reflected clusters during the interval from November to August in the approximate $[X, Y]$ regions [22,1–6] and [20–23,11–17] was taken as evidence of the presence of multiple disease foci within the field (Fig. 5B). These data, in conjunction with the absence of reflected clusters during the previous interval (November to July), were evidence that the process of establishment of secondary foci of symptomatic plants had begun between July and August 1993. The lower values for core cluster size and proximity index for disease increase from November to August compared with values for disease increase from November to July were indications that increase of papaya ringspot to proximal plants was less likely during the interval from November to August than from November to July.

A significant edge effect was detected for disease increase during assessment intervals from February to August 1993 and March to August 1993, indicating that newly diseased plants were likely to be found at the edge of the field (Table 1, Figs. 4 and 5C and D). The size of the core cluster for increase of papaya ringspot from February to August was much larger than from March to August (15 and 2, respectively) (Table 1, Fig. 5C and D), indicating that the probability of symptoms of papaya ringspot developing on plants adjacent to diseased plants was low during the period from March to August. The larger size of the reflected clusters in the period from February to August compared with the period from November to August was taken as evidence that between February and August increase in symptom expression occurred within and around secondary disease foci rather than within and around the original (primary) focus of papaya ringspot. The larger size and proximity of reflected clusters (Fig. 5D) in the period from March to August compared with the period from February to August was taken as evidence of coalescence of secondary foci.

DISCUSSION

Spatial patterns of disease in plant populations reflect underlying interactions of biological and physical processes among host

TABLE 1. Summary statistics for spatiotemporal distance class analysis of citrus variegated chlorosis in Brazil during 1989–1992 and an epidemic of papaya ringspot on Oahu, Hawaii, during 1992–1993

Assessment interval	Disease incidence[a] (%)	SCF+[b]	SCF−[c]	Pattern of disease increase[d]	Core size[e]	Proximity index[f]	Reflected clusters		Edge effect[g]
							Number	Size	
Citrus variegated chlorosis									
1989–1990	13–25	0.16	0.20	A	131	0.64	3	2	ns
1990–1991	25–50	0.11	0.13	A	97	0.71	2	2	ns
1991–1992	50–64	0.25	0.09	A	1	...	4	2–216	ns
Papaya ringspot									
November–July	9–20	0.09	0.03	A	39	0.52	0	0	ns
November–August	9–21	0.09	0.03	A	25	0.46	4	2–7	ns
February–August	12–21	0.08	0.02	A	15	0.37	3	2–8	s
March–August	15–21	0.09	0.03	A	2	1.00	3	2–16	s

[a] Percentage of symptomatic plants at the beginning and end of the disease assessment interval, respectively.
[b] Proportion of $[X, Y]$ distance classes with standardized count frequency (SCF) significantly greater than expected ($P \leq 0.05$) compared with a random distribution of newly diseased plants.
[c] Proportion of $[X, Y]$ distance classes with SCF significantly less than expected ($P \geq 0.95$).
[d] A = aggregated (nonrandom) pattern.
[e] Number of contiguous distance classes with significant SCF values ($P \leq 0.05$) within the $X \times Y$ dimensions of the core cluster; represents the core zone of disease increase in relation to previously diseased plants.
[f] Measure of the density of newly diseased plants in the core cluster calculated as the number of significant SCF values in the core cluster/$X \times Y$ dimensions of the core cluster. The index is not calculated when core cluster size = 1.
[g] ns = Not significant, and s = significant.

and pathogen(s) in a complex environment. Methods of descriptive and quantitative pattern analysis provide insight into potential cause and effect relationships in the increase of disease within plant populations. Spatiotemporal distance class analysis permits both a simple description of disease increase and a way to detect nonrandomness and quantify attributes of disease increase and clustering. The analysis also identifies important times of disease increase, providing more insight into events that may have led to the observed patterns in space and time.

The citrus variegated chlorosis data set presented herein is a relatively small subset of the entire citrus grove studied but does include the original focus of disease. The strong indication of disease increase to adjacent plants both within and across tree rows (in the original and secondary disease foci) implies a contagious process that may involve a vector and suggests the need for more data on the ecology of the causal agent and potential vector(s). The evidence for the establishment of secondary foci suggests the need for management strategies designed to reduce the probability of the establishment and expansion of multiple foci.

The papaya ringspot epidemic was selected to demonstrate the ability of spatiotemporal distance analysis to analyze disease assessments in overlapping intervals. This is a viable, albeit indirect, approach to analyzing data sets with minimal increases in disease incidence between assessments. Papaya ringspot data also portray a spatial chain of events that occurred during the epidemic. A conceptual model of such a chain of events could be as follows: 1) the establishment of an initial focus of disease within a field; 2) the "filling in" and radial expansion of the initial focus; 3) the establishment of secondary foci; 4) the filling in and expansion of secondary foci; and 5) the coalescence of initial and secondary clusters and establishment of tertiary foci. Some of the events within this conceptual model were identified within the papaya field. For example, a comparison of distance class matrices for disease increase from November to July and November to August (Fig. 5A and B, respectively) revealed that

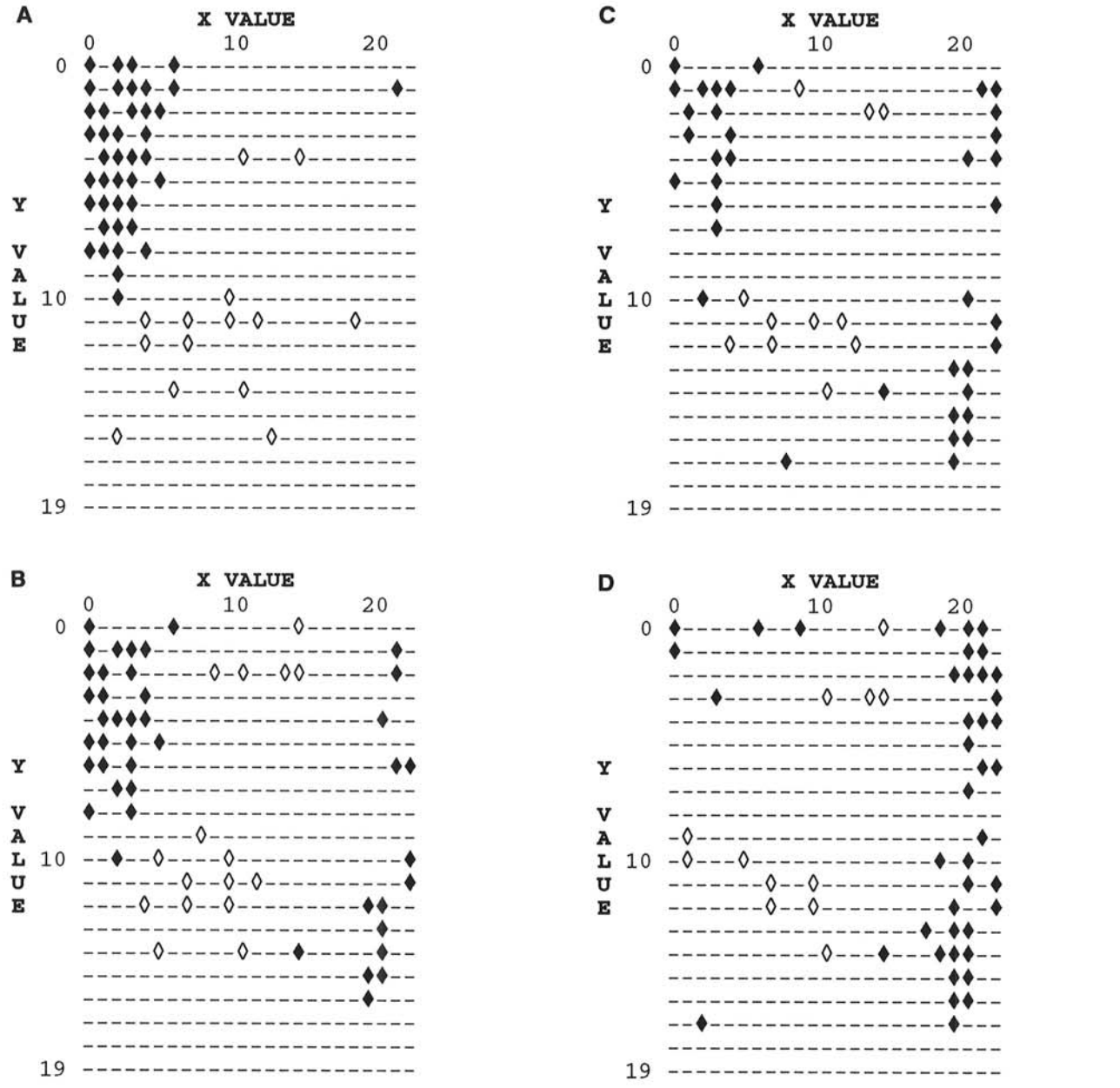

Fig. 5. Distance class matrices from spatiotemporal distance class analysis of an epidemic of papaya ringspot in Hawaii representing patterns of disease increase from **A,** November 1992 to July 1993, **B,** November 1992 to August 1993, **C,** February to August 1993, and **D,** March to August 1993. ◆ = $[X, Y]$ distance class with standardized count frequency (SCF) significantly greater than expected ($P \leq 0.05$); ◇ = $[X, Y]$ distance class with SCF significantly less than expected ($P \geq 0.95$); and − = $[X, Y]$ distance class with nonsignificant SCF value.

reflected clusters were detected during the interval from November to August and not in the data from November to July (direct analysis of disease increase from July to August was not possible, given that the analytical criterion of a 10% increase in disease increase between assessments was not satisfied). This was taken as evidence for the establishment of secondary clusters of symptomatic plants between July and August. A comparison of distance class matrices for disease increase from February to August and from March to August (Fig. 5C and D, respectively) revealed a large difference in core cluster size between the two intervals. The reduced core cluster for the interval from March to August in relation to the interval from February to August (and the larger reflected clusters) indicated that by March, most of the spatial positions in the initial disease focus had become occupied by diseased trees and that the increase in symptomatic plants was occurring to and within secondary foci in the field. Therefore, by maintaining as constant either the first date of comparison (Fig. 5A and B) or the second date (Fig. 5C and D), information about the time and relative locations of epidemiologically important events was derived.

Attributes of the distance class matrices also revealed information that potentially could be linked to the biology and ecology of epidemic processes and suggested further hypotheses to be tested. The long axes of the core and reflected clusters in the papaya ringspot analysis (Fig. 5) were parallel to the direction of agronomic rows. Thus, there was a greater probability of disease increase within, rather than across, rows in this field, a phenomenon possibly attributable to closer between-tree spacing within rows than across rows. No evidence for exchange of inoculum between the two papaya fields was observed. Disease incidence remained <1% in the adjacent field, and symptomatic plants were not observed until many months after the initial disease focus was observed in the planting of papaya used in the analysis (data not shown). These data (in addition to the remoteness of the location) suggest that the epidemic was being driven exclusively by within-field increase of papaya ringspot. The spatial locations of reflected clusters and diseased plants by August indicated a high probability of disease increase to plants relatively removed from previously diseased plants. These data may reflect the feeding behavior of the aphid vector(s). Papaya is not a preferred host for the species of aphid vectors (S. A. Ferreira, *personal communication*). Thus, after probing diseased plants, the aphid vectors likely were motivated to fly from infected plants to more distal locations.

Spatiotemporal distance class analysis represents a potentially important approach to the study of spatial pattern in plant disease epidemiology. The method could be used as a comparative tool to investigate disease increase and management by providing a quantification of patterns resulting from management strategies (e.g., roguing and vector disruption). The method may be applied to any biological or physical system in which binary data are relevant simplifications of the system.

Forms of data analysis, including the one described herein, have inherent limitations, suggesting that a carefully selected combination of techniques would optimize analytical power. Spatiotemporal distance class analysis is largely a descriptive method and thereby differs from mechanistic forms in intent and application. Spatiotemporal distance class analysis is not intended to identify models that can account for the evolution of observed spatial patterns (unlike spatiotemporal autocorrelation analysis [12,13]), nor is the analysis intended to provide an integrated, simultaneous evaluation of an entire epidemic (unlike spatiotemporal autocorrelation analysis). Rather, it is limited to specific comparisons between disease assessment dates. Strictly speaking, the use of spatiotemporal distance class analysis does not allow attachment of a Type I error rate to assertions about pattern development in space and time (unlike distribution fitting procedures, for example). The analysis may be more applicable at an individual plant basis that at the level of a population in a quadrat. The preceding limitations suggest the need to examine spatiotemporal data from different perspectives.

The strengths and capabilities of spatiotemporal distance class analysis lend credence to its use in an integrated approach to disease data analysis. The conservative nature of the decision criteria (e.g., the significance of SCF values) imitates that of more formal statistical tests (e.g., *t* tests and chi-square) and protects against false conclusions. Spatiotemporal distance class analysis conserves information on plant location. The method is independent of quadrat size and shape relative to distribution-fitting procedures, sparse sampling techniques, and some descriptive statistics (e.g., indices of dispersion). Thus, experimental design and data analysis are relatively independent of questions and problems concerning optimum quadrat size and/or shape (1). Incidence of disease is recorded for individuals as spatially distinct units rather than for a population of individuals within spatially distinct quadrats, thereby distinguishing the technique from forms of quadrat data analysis. Spatiotemporal distance class analysis has the potential to provide insight into pathogen and host ecology. Determinants of pathosystem behavior may be reflected in edge effects, cluster size and shape and direction and magnitude of expansion, and the location and time of the establishment of secondary foci. The method is self-contained and relatively simple; i.e., no prior knowledge of the statistical theory of arguably more complex concepts such as geostatistics or time-series analysis is necessary. Finally, the analysis is not limited to consecutive disease assessments. This allows a more flexible pattern analysis to be conducted at different levels of temporal resolution (potentially important if the disease latent period is unknown).

LITERATURE CITED

1. Campbell, C. L., and Madden, L. V. 1990. Introduction to Plant Disease Epidemiology. John Wiley & Sons, New York.
2. Chang, C. J., Garnier, M., Zreik, L., Rossetti, V., and Bove, J. M. 1993. Culture and serological detection of the xylem-limited bacterium causing citrus variegated chlorosis and its identification as a strain of *Xylella fastidiosa*. Curr. Microbiol. 27:137-142.
3. Filajdić, N., and Sutton, T. B. 1993. Spatial pattern of Alternaria blotch of apple (Abstr.) Phytopathology 83:1391.
4. Frisina, T. A., and Benson, D. M. 1989. Occurrence of binucleate *Rhizoctonia* spp. on azalea and spatial analysis of web blight in container-grown nursery stock. Plant Dis. 73:249-254.
5. Gottwald, T. R., Gidtti, F. B., Santos, J. M., and Carvalho, A. C. 1993. Preliminary spatial and temporal analysis of citrus variegated chlorosis in Brazil. Pages 327-355 in: Proc. Conf. Int. Org. Citrus Virol., 12th. P. Moreno, J. V. DaGraca, and L. W. Timmer, eds. IOVC, Riverside, CA.
6. Gray, S. M., Moyer, J. W., and Bloomfield, P. 1986. Two-dimensional distance class model for quantitative description of virus-infected plant distribution lattices. Phytopathology 76:243-248.
7. Gray, S. M., Moyer, J. W., Kennedy, G. G., and Campbell, C. L. 1986. Virus-suppression and aphid resistance effects on spatial and temporal spread of watermelon mosaic virus 2. Phytopathology 76:1254-1259.
8. Lee, R. F., Derrick, K. S., Beretta, M. J. G., Chagas, C. M., and Rossetti, V. 1991. Citrus variegated chlorosis: A new destructive disease of citrus in Brazil. Citrus Ind. 72:12-13, 15.
9. Munkvold, G. P., Duthie, J. A., and Marois, J. J. 1993. Spatial patterns of grapevines with Eutypa dieback in vineyards with or without perithecia. Phytopathology 83:1440-1448.
10. Nelson, S. C. 1992. Spatial and temporal ecology of pathogens in a foliar disease complex on white clover. Ph.D. thesis. North Carolina State University, Raleigh.
11. Nelson, S. C., and Campbell, C. L. 1993. Comparative spatial analysis of foliar epidemics on white clover caused by viruses, fungi, and a bacterium. Phytopathology 83:288-301.
12. Nelson, S. C., Marsh, P. L., and Campbell, C. L. 1992. 2DCLASS, a two-dimensional distance class analysis software for the personal computer. Plant Dis. 76:427-432.
13. Reynolds, K. M., and Madden, L. V. 1988. Analysis of epidemics using spatio-temporal autocorrelation. Phytopathology 78:240-246.
14. Reynolds, K. M., Madden, L. V., and Ellis, M. A. 1988. Spatio-temporal analysis of epidemic development of leather rot of strawberry. Phytopathology 78:246-252.
15. Ristaino, J. B., Larkin, R. P., and Campbell, C. L. 1993. Spatial and temporal dynamics of Phytophthora epidemics in commercial bell pepper fields. Phytopathology 83:1312-1320.